



UNIVERSITEIT•STELLENBOSCH•UNIVERSITY
jou kennisvennoot • your knowledge partner

Stochastic inversion of fire test data for the T-dependant thermal diffusivity of SA pine

by

Liza Stewart
21555575

Project(Civil Engineering)458

Final Draft

Study leader: Prof N de Koker

October 2021

Contents

Contents	i
List of Figures	iii
List of Tables	iv
Nomenclature	v
1 Introduction	1
1.1 Background and Motivation	1
1.2 Aim and objectives	2
1.3 Literature study	3
2 Technical Foundation	4
2.1 Finite Element Method	4
2.1.1 Origin	4
2.1.2	4
2.1.3 Heat diffusion	4
2.1.4 Heat conduction	5
2.2 Bayes' theorem of inverse problems	5
2.3 Markov Chain Monte Carlo	5
2.3.1 Markov Chains	5
2.3.2 Monte Carlo Integration	7
2.3.3 Metropolis-Hastings Algorithm	7
2.4 Thermal properties of timber	7
3 Implementation	8
3.1 Existing data	8
3.1.1 Summary of test	8
3.1.2 Potential inaccuracies	10
3.2 Finite Element Modelling	10
3.2.1 Derivation	11
3.2.2 Existing Model	16
3.2.3 Adapted Model	17

3.3	Inversion method	17
3.3.1	Prior probability	17
3.3.2	Likelihood probability function	18
3.3.3	MCMC integration	19
4	Results	20
4.1	Resulting k-values	20
4.2	Model output	22
5	Discussion	23
6	Summary and Conclusion	24
A	Relevant code segments	25
B	Detailed results graph	27
C	Derivation	29
D	Program	32
E	GA outcomes	33
	List of References	35

List of Figures

1.1	Standard temperature-thermal conductivity relationship for timber from (CEN, 2004)	2
2.1	Three-dimensional example of Markov Chain application (Created on https://www.geogebra.org/3d)	6
3.1	Thermocouple layout in test conducted by van der Westhuyzen <i>et al.</i> (2020) cross-section (left) and overall layout (right)	9
3.2	Standard ISO fire curve TODO	9
3.3	Visualisation of element that is modelled in one-dimension	11
3.4	Visualisation of one-dimensional element with air elements and external conditions added	12
3.5	Output of finite element model using κ -values as indicated in EN 1995:1-2-2004	17
3.6	Graph explaining the difference in acceptance rates (Generated at https://www.geogebra.org/graphing/g7kyzwce)	19
4.1	Resulting κ values (left) compared to Euro-code standard values(right)	21

List of Tables

Nomenclature

Constants

$$g = 9.81 \text{ m/s}^2$$

Variables

κ	Thermal conductivity	[W/m·K]
α	Thermal diffusivity	[m ² /s]
c_ρ	Heat capacity	[J/kg/K]

Chapter 1

Introduction

This chapter will introduce the problem addressed in this project. Previous similar projects as well as the value of this research will also be addressed.

1.1 Background and Motivation

Traditionally the thermal conductivity, otherwise referred to as the κ -value, of timber is based simply off the EN 1995:1-1-2004 or similar standards. This research project will aim to obtain the thermal diffusivity of cross laminated SA-Pine timber by further analysing data obtained by S. van der Westhuyzen for his study of the samples' charring rate.

The thermal diffusivity of timber is a unobservable quantity that cannot be measured directly. Instead, it is related to measurements of temperature and time through differential models. When heat diffusion is calculated using Finite Element methods(TODO:choose which FEM), the process is usually simplified to a linear problem (Fish, 2007). Due to the changes in thermal diffusivity of timber with temperature, as can be seen in EN 1995:1-1-2004(pg number T) and Figure 3.32, the diffusivity cannot be linearly modelled. Therefore, the problem lends itself to being analysed by inversion techniques. The aforementioned approach will allow us to obtain information about the diffusivity based on the combination of the information assumed prior to measuring, further referred to as the prior, and the measured data. Using statistical inversion leads to a probability distribution that provides us with a collection of diffusivity estimates and their corresponding probabilities.

Currently the fire rating of specific timber samples are based on fire tests conducted in a furnace. The furnace is kept at increasing temperatures corresponding with the Standard or ISO 834 fire curve as specified in ISO 834 ISO (1999). This process becomes very costly if it has to be repeated every time that timber is used for construction, as timber usage for multiple story construction projects have increased over the past decades. This increase is

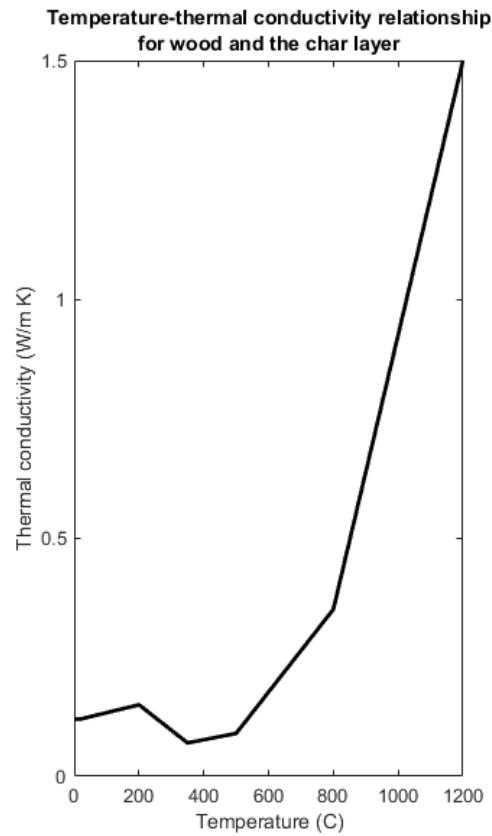


Figure 1.1: Standard temperature-thermal conductivity relationship for timber from (CEN, 2004)

partially due to the sustainability of timber as a construction material: not only is it renewable but it also has a small carbon footprint (Salvadori, 2017). Obtaining and standardising different thermal diffusivity values for different species of timber, will assist in more accurate modelling. If modelling accuracy can be increased, the option to use modelling as either confirmation of fire tests or instead of small scale fire test will become more feasible.

/

1.2 Aim and objectives

During the course of the project, the student will aim to meet the following objectives:

1. Modify a Finite Element Model into an accurate and effective function;
2. Compare the model data to the actual acquired data;

3. Solve for the thermal diffusivity using Bayes' theorem of inverse problems; and
4. Evaluate and explore the posterior probability distribution using the following methods:
 - (a) Maximum a Posteriori
 - (b) Markov-Chain Monte Carlo

1.3 Literature study

In their article *Simple Method to Determine the Diffusivity of Green Wood*, Frayssinhes *et al.* determine the global diffusivity of a Douglas fir green log using inverse identification methods. Their experiment was set up by immersing the log with K-type thermocouples into a boiler filled with water at 60°C. These K-type thermocouples were very specifically placed to improve the accuracy of the diffusivity ratio calculation. The finite element model constructed for their calculations used linear interpolation with four node quadrangle elements. An analytical model was also constructed using the heat propagation equation (TODO?heat diffusion?). The intent of this research was to assist the peeling industry in making the pretreatment process more cost effective. The method proved to be effective at determining the thermal diffusivity of green Douglas fir logs, as the κ -values obtained were comparable to those from literature. The methods used by Frayssinhes *et al.* (2020) are similar to the methods described later in the report. A crucial difference remains as the temperatures at which these experiments were conducted as well as the final usage of the data differ greatly.

All the thermal properties of various timber species at high temperatures were discussed in an article by Shi and Chew (2021).

Chapter 2

Technical Foundation

2.1 Finite Element Method

Finite element methods (or finite element analysis) is used when the behaviour of an element cannot be accurately depicted by a simple mathematical equation.

2.1.1 Origin

The finite element method (FEM) used today is the sum of decades of research. In an article by Gupta and Meek they discuss the five main contributors to the finite element method. According to Gupta and Meek (1996) the idea behind the finite element method was initially explored in the 1943 article by Courant. Courant acknowledges the complex nature of mathematical problems in his first paragraph by stating: "Mathematics is an indivisible organism uniting theoretical contemplation and active application." He goes on to discuss the variational method created by (Ryes?)

2.1.2

A larger element is broken into smaller elements. Assumptions made on the smaller scale have a lesser effect on the final answer than the same assumptions made on a large scale would have had.

2.1.3 Heat diffusion

In its simplest form, the one-dimensional heat diffusion equation is a partial differential equation 2.1 dependant on the temperature and thickness of the element. The heat diffusion equation is based on Fourier's Law...(TODO)

$$q = -k \frac{dT}{dx} \quad (2.1)$$

2.1.4 Heat conduction

TODO: - Explain Galerkin Weak form, Newmann boundaries and Dirichlet Boundaries

2.2 Bayes' theorem of inverse problems

The method of statistical inversion is dependant on a fundamental understanding of the Bayes' theorem of inverse problems. The student obtained this understanding through studying Chapter 3 of statistical and Computational Inverse problems by Kaipio and Somersalo (2005), further referred to merely as Kaipio. There are four principles of Statistical inversion that is essential to the thorough understanding of these models. Firstly, it is the principle that any variable in the model needs to be modelled as a random variable. This randomness is based on the extent of information that is available. To ensure that the extent of knowledge is accurately portrayed in the model, the extent of knowledge will be coded into the probability distributions assigned to the different variables. Finally, it needs to be understood that the solution of a statistical inversion is a posterior probability distribution. A generalized equation of Bayes' theorem can be seen in 2.2 taken from Kaipio.

$$\pi_{\text{post}}(x) = \pi(x|y_{\text{observed}}) = \frac{\pi_{\text{pr}}(x)\pi(y_{\text{observed}}|x)}{\pi(y_{\text{observed}})} \quad (2.2)$$

2.3 Markov Chain Monte Carlo

Markov Chain Monte Carlo (MCMC) is a method of integration which will be used to determine the mean of the κ -values at specific temperatures. Markov Chain Monte Carlo is a method that was created by combining the concept of Monte Carlo sampling and a Markov Chain. To fully understand MCMC, its underlying methods must be investigated further. For a better understanding of this concept, *Introducing Markov chain Monte Carlo* by Gilks *et al.*, Kaipio, and various websites Brownlee (2019), Wiecki (2015) were consulted. (RIJK: is sin lomp?)

2.3.1 Markov Chains

The core principle of a Markov chain is that the next value (x_{n+1}) in a sequence is dependent on the current value (x_n). A step size that indicates the range

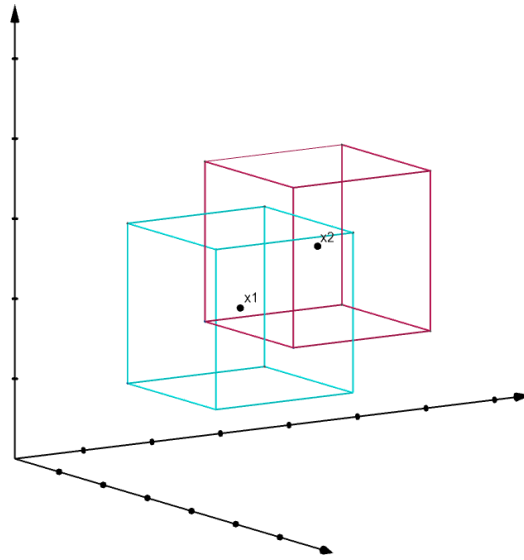


Figure 2.1: Three-dimensional example of Markov Chain application (Created on <https://www.geogebra.org/3d>)

from the initial point that the next falls in is chosen. Values are then randomly generated but restricted to be within this range. This concept can be visualised as follows: our accepted point (x_1) is in the center of a cube. The next possible random point is randomly generated but still within the cube (our search range). After this next number is selected, the cube moves such that the new point (x_2) is now the centre, and so it continues. See Figure 2.1 for clarification. The above example simplifies the concept, but this understanding can now be expanded. If every coordinate direction in the aforementioned simple example is seen as a single entry in the x vector, then the example has three independent values. More or less values can be used depending on the problem. Another level of complication can be added if it is taken into account that every point in the cube is no longer equally likely. A distribution within the cube can be chosen, for example simply a normal distribution. The shape of the cube then warps into a stranger shape with points closer to the center being more likely choices and the edges being less likely.

The purpose of a Markov Chain is for the chain to converge to a distribution and be independent on the very initial estimation. In principle it should then reach a near stationary distribution. Since Markov Chains are not used if we know the answer, a way to determine when values are no longer affected by the initial estimate is needed Gilks *et al.* (1996). The simple proposed solution is the concept of burn-in. The concept of conventional burn-in for usage in Markov Chains are disputed as the Markov Chain itself is created in such a way that values are only directly dependent on the value immediately before them

Meyn and Tweedie (1993). Burn-in in the Markov Chain sense can simply be referred to as the removal of the initial samples of low probability to increase the accuracy of the average taken after all the iterations Cook (2016).

2.3.2 Monte Carlo Integration

Monte Carlo integration is used to evaluate a probability distribution that cannot be solved simply. The evaluation is done by drawing a collection of random values from the distribution. These values are then used as the sample, and a sample mean is taken. The arithmetic sample mean can be used to approximate the population mean in accordance with the law of large numbers (Gilks *et al.*, 1996). All of the random samples generated can not be immediately accepted. Here, the acceptance criteria comes into play. There are multiple options for how a posterior is deemed acceptable; these are elaborated on in the book *Monte Carlo Statistical Methods* by Robert and Casella. The most general acceptance criteria is set out in Equation 2.3 and comes from Kaipio.

$$\begin{aligned}
 &\text{if } \frac{\pi(x_2)}{\pi(x_1)} > 1 \quad \text{Accept automatically} \\
 &\text{or } \frac{\pi(x_2)}{\pi(x_1)} > \text{rand} \quad \text{Accept} \\
 &\text{else reject and reselect } x_2
 \end{aligned} \tag{2.3}$$

2.3.3 Metropolis-Hastings Algorithm

The Metropolis-Hastings algorithm is one of the available simulation methods based on the MCMC principles. For the purposes of this project the Metropolis-Hastings algorithm was chosen above the Gibbs-sampler TODO

2.4 Thermal properties of timber

Chapter 3

Implementation

This chapter will elaborate on the test data used as well as the process that was followed to achieve the results in Chapter 4.

3.1 Existing data

The data used was acquired by van der Westhuyzen *et al.* (2020) for an article assessing the charring rate of both SA-Pine and Eucalyptus. For the purpose of this project, only the data obtained from the SA-Pine test was considered and analysed.

3.1.1 Summary of test

The test was conducted on a sample panel of 100 mm by 0.9 m \times 0.9 m cross-laminated SA-pine. This sample was then divided into nine cubes of 100 mm \times 100 mm \times 100 mm. Each cube was fitted with seven Type K-thermocouples placed at consecutive 16.5 mm drilled holes, as can be seen in Figure 3.1. The test panel was tested in a furnace and was exposed to the standard ISO 834 Fire curve 3.2 on one side and room temperature on the other. The panel was exposed to the fire curve for 50 minutes, at which stage near complete de-lamination was observed and the test ended.



Figure 3.1: Thermocouple layout in test conducted by van der Westhuyzen *et al.* (2020) cross-section (left) and overall layout (right)

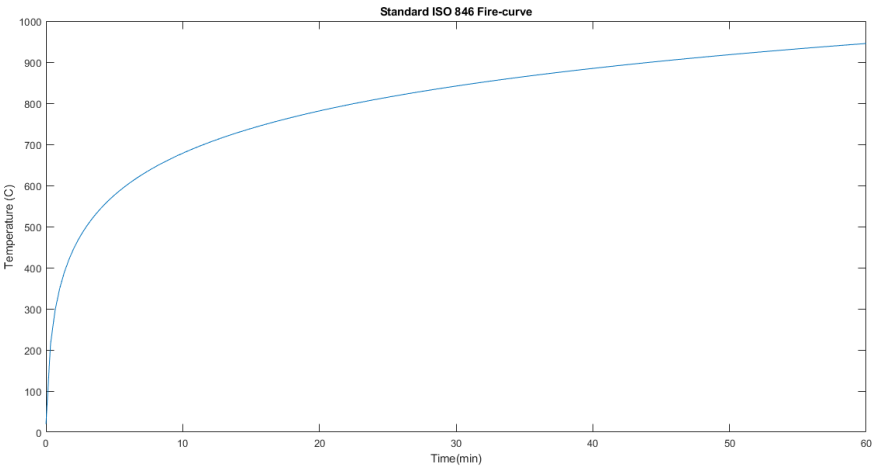
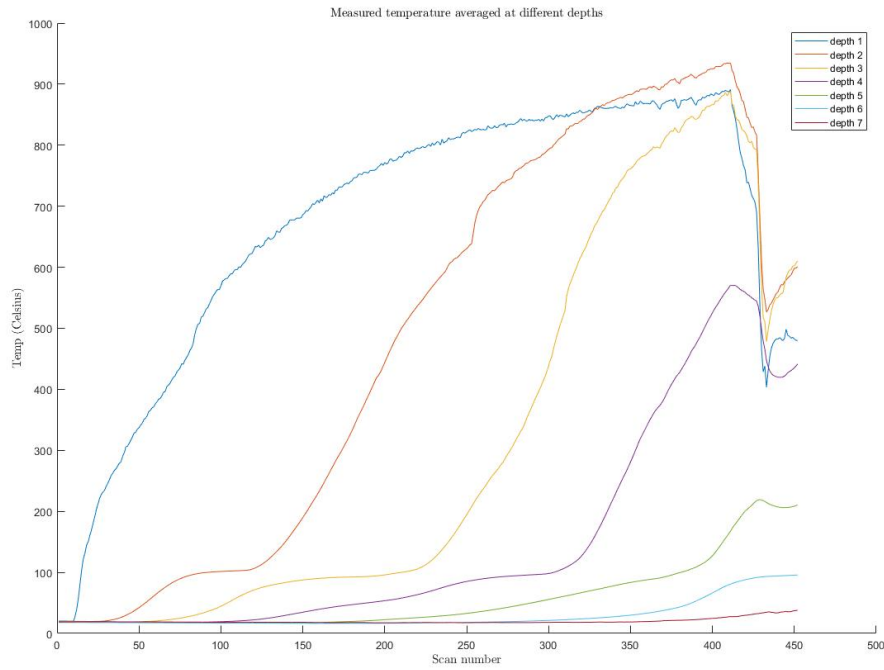


Figure 3.2: Standard ISO fire curve TODO

In Figure 3.1.1



3.1.2 Potential inaccuracies

As with most tests, everything is not always perfect. The potential inaccuracies are discussed below. In the data, it was observed that two of the thermocouples broke during testing; this resulted in temperature with a magnitude of 10^{13} . Such a temperature is impossible, as the highest ever recorded temperature reached was 4×10^{12} and that only occurred in a atomic explosion. This malfunction required that two of the depth measurements were no longer the average between nine samples but instead the average between eight. Another inaccuracy that could potentially influence the accuracy of the final result is the accuracy of the depth of the holes in which the thermocouples were placed.

There is also debate about the significance of the contribution of the timber burning to the temperature inside the furnace. For the purposes of this project, it will be assumed that the timber burning does not contribute to the temperature inside the furnace.

3.2 Finite Element Modelling

A one-dimensional finite element model that simulates what we expect to obtain from the fire tests based on the simplified κ -values provided in EN 1995:1-2-2004 is modified into a function. This function should provide the

temperature of the modelled element based on a specified location and thermal conductivity. The derivation and adaptation of the model are expanded on below.

3.2.1 Derivation

Assumptions were made to simplify the model, they were as follows

1. The air on the side of fire follows the temperature of the fire curve.
2. The air on the cold side remains at 20°C.

Stationary heat conduction

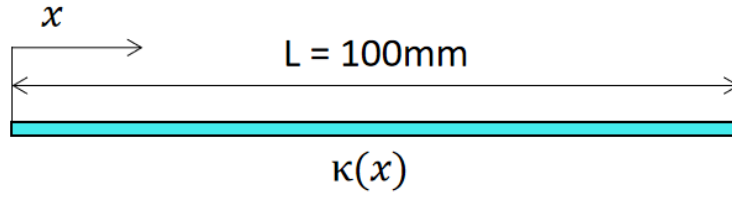


Figure 3.3: Visualisation of element that is modelled in one-dimension

The derivation started as a one-dimensional stationary heat conduction problem with the below equations as a starting point.

$$q_{,x} - f = 0 \dots(1) \qquad q = -\kappa u_{,x} \dots(2) \qquad (3.1)$$

Integrating Equation 3.1 (1) over the length of the element (shown in Figure 3.2.1) and introducing a weighting function $w(x)$ we obtain 3.2. Since the derivative of $w(0)$ is known and $q_{,x}$ is unknown. The first term in 3.2 is integrated by parts. After the integration by parts and substituting q with 3.1 (2), Equation 3.3 is created.

$$\int_{x=0}^L w q_{,x} dx - \int_{x=0}^L w f dx = 0 \qquad (3.2)$$

$$\int_{x=0}^L w \kappa u_{,x} dx + \int_{x=0}^L w f dx - w q|_0^L = 0 \qquad (3.3)$$

In Equation 3.3 the u and w need to be defined. Assuming $u \approx u^h$ and $w \approx w^h$ and using the basis function (N^A), Equation 3.4 is obtained.

$$\begin{aligned} u_e^h &= \sum_B N^B d^B \quad ; \quad w_e^h = \sum_A N^A c^A \\ u_{e,x}^h &= \sum_B N_{,x}^B d^B \quad ; \quad w_{e,x}^h = \sum_A N_{,x}^A c^A \end{aligned} \quad (3.4)$$

Substituting the u and w functions back, we obtain the Galerkin weak form shown in Equation 3.5. In Equation 3.5 the A_N refers to the nodes that have Newmann boundaries (TODO explained in 2.1). The variables c^A and d^B are independent of x and can therefore be taken out of the integral. The sum over A and B are also taken out of the integral. When the summing is applied a matrix of all the possible combinations between A and B can be used to replace the sum. The resulting matrices are shown in Equation 3.6. When written in matrix form the summing is implied, if matrix form is it written then the expression refers to the terms that will still be summed.

$$\begin{aligned} \sum_e \int_{\Omega_e} w_{e,x}^h k u_{e,x}^h dx + \sum_e \int_{\Omega_e} w_e^h f dx - w(L)q_L + w(0)q_0 &= 0 \\ \int_{\Omega_e} \sum_A \sum_B N_{,x}^A c^A k N_{,x}^B d^B dx + \int_{\Omega_e} \sum_A N^A c^A f dx - \sum_{A \in A_N} c^A q^A &= 0 \end{aligned} \quad (3.5)$$

$$\mathbf{c}_e^T \mathbf{K}_e^{AB} \mathbf{d}_e + \mathbf{c}_e^T \mathbf{F}_e^f - \mathbf{c}_e^T \mathbf{F}_e^q \quad (3.6)$$

where

$$\begin{aligned} K_e^{AB} &= \int_{\Omega_e} N_{,x}^A N_{,x}^B k dx \\ F_e^{Af} &= \int_{\Omega_e} N_{,x}^A f dx \\ F_e^{Aq} &= \begin{cases} q(x_N) & \text{for } x \in \Gamma_N \\ 0 & \text{for other} \end{cases} \end{aligned}$$

Boundaries

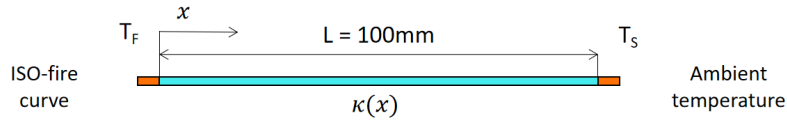


Figure 3.4: Visualisation of one-dimensional element with air elements and external conditions added

One of the additional difficulties in modelling is that the known boundary temperatures are measured in the air of the furnace and assumed for the air outside the furnace. Initially a long element of air was modelled. This element is then overlaid with the timber element to effectively add an air element at each end of the timber element as depicted in 3.2.1. In the air elements, both heat convection and heat radiation need to be taken into account. The equations for heat convection and radiation can be seen in Equation 3.7 and 3.8.

$$q_{\text{adv}} = \nu \rho c_p \Delta T = h \Delta T$$

ν = velocity m/s
 ρ = density of air
 c_p = heat capacity of air

(3.7)

$$q_{\text{rad}} = \varepsilon \sigma \phi (T_f^4 - T_s^4)$$

ε = emissivity
 σ = Stefan-Boltzmann
 $5.670e-8 [W/(m^2 K^4)]$
 ϕ = view factor; 1 here

(3.8)

Given that T_s and T_f are known a new equivalent heat flux value can be calculated as in Equation 3.9.

$$q_{\text{con}}^{\text{equiv}} = \kappa^{\text{equiv}} \frac{\Delta T}{\Delta L} = q_{\text{rad}} + q_{\text{adv}} \quad (3.9)$$

Due to the clear relationship between heat flux and thermal diffusivity the equivalent diffusivity (κ^{equiv}) can be calculated as shown below in Equation 3.10.

$$\begin{aligned} \kappa^{\text{equiv}} &= \frac{[q_{\text{rad}} + q_{\text{adv}}]}{\Delta T} \\ &= \frac{\varepsilon \sigma \phi \Delta (T^4)}{\Delta T / \Delta L} + h \Delta L \\ &= \frac{\varepsilon \sigma \Delta (T^4)}{\Delta T} + h \end{aligned} \quad (3.10)$$

One-dimensional diffusion

The concept of diffusion is thoroughly explained in 2.1(TODO) below the mathematical application is explained and steps that were taken to obtain the final model is shown.

$$q_{,x} - f = \frac{\partial Q}{\partial t} = c_p \frac{\partial u}{\partial t} \quad \dots(1) \qquad q = -\kappa \frac{\partial u}{\partial x} \quad \dots(2) \quad (3.11)$$

Substituting Equation 3.11(2) into 3.11 and taking the derivative as indicated ($q_{,x}$) gives Equation 3.12. As previously discussed heat conduction (α) is heat diffusion (κ) divided by specific heat (c_p).

$$\begin{aligned} \therefore -\kappa \frac{\partial^2 u}{\partial x^2} - f &= c_p \frac{\partial u}{\partial t} \rightarrow f = 0 : \\ \frac{\partial^2 u}{\partial x^2} &= -\frac{c_p}{\kappa} \frac{\partial u}{\partial t} \\ \text{or} \\ \frac{\partial u}{\partial t} &= -\alpha \frac{\partial^2 u}{\partial x^2} \end{aligned} \quad (3.12)$$

Let $c_p = \lambda$

$$\therefore -\kappa u_{,xx} - \lambda u_{,t} = f \quad (3.13)$$

Then:

$$\int_0^L w q_{,x} dx - \int_0^L w \lambda u_{,t} dx - \int_0^L w f dx = 0 \quad (3.14)$$

Similar to what was done in 3.4 a special approximation is made to obtain Equation 3.15.

$$u \approx u^h \rightarrow u_e^h = \sum_A N^A d^A \quad ; \quad w_e^h = \sum_A N^A L^A \quad (3.15)$$

$$\rightarrow \sum_e \int_{\Omega^e} w_{e,x}^h \kappa u_{e,x}^h dx_e + \sum_e \int_{\Omega^e} w_e^h \lambda u_{e,t}^h dx_e + \sum_e \int_{\Omega^e} w_e^h f dx_e - \sum_{e \in \epsilon_A} w q_N = 0 \quad (3.16)$$

$$*_1 : \int_{\Omega^e} \sum_A \sum_B N_{,x}^A c^A \kappa N_{,x}^B d^B dx = \sum_A \sum_B \left[\int N_{,x}^A N_{,x}^B \kappa dx \right] d^B = \mathbf{c}_e^T \boldsymbol{\kappa}_e \mathbf{d}_e$$

$$*_2 : \int_{\Omega^e} \sum_A \sum_B N^A c^A \lambda N^B \dot{d}^B dx = \sum_A \sum_B c^A \left[\int N^A N^B \lambda dx \right] d^B = \mathbf{c}_e^T \mathbf{M}_e \dot{\mathbf{d}}_e$$

$$*_3 : \int_{\Omega^e} \sum_A N^A c^A f dx = \sum_B c \int_B N f dx = \mathbf{c}_e^T \mathbf{F}_e^B$$

$$*_4 : \sum_{A \in \mathcal{A}} \kappa^A q_N^A = \mathbf{c}_e^T \mathbf{F}_e^q$$

From all the above equations the below matrix formulation could be assembled:

$$\mathbf{c}^T \boldsymbol{\kappa} \mathbf{d} + \mathbf{c}^T \mathbf{M} \dot{\mathbf{d}} = \mathbf{c}^T \mathbf{F} \quad (3.17)$$

Solving:(TODO: date 15/10 last)

$$(1) \text{ Set } \mathbf{d}_0 = |---|---|---| \& \mathbf{v}_0 = \mathbf{0} \text{ Also set } \alpha \text{ (mixing constant?); } \Delta t \quad (3.18)$$

$$(2) \text{ Time integration [v-form; Hughes Ch8] } \mathbf{d}_{n+1} = \mathbf{d}_n + (1 - \alpha) \Delta \mathbf{v}_n + \alpha \Delta t \mathbf{v}_{n+1} \quad (3.19)$$

$$(\mathbf{M} + \alpha \Delta t \boldsymbol{\kappa}) \mathbf{v}_{n+1} = \mathbf{F}_{n+1} - \boldsymbol{\kappa} \tilde{\mathbf{d}}_{n+1} \quad (3.20)$$

if \mathbf{M} and $\boldsymbol{\kappa}$ independent of time and temperature, sufficient to say:

$$\mathbf{v}_{n+1} = (\mathbf{M} + \alpha \Delta t \boldsymbol{\kappa})^{-1} (\mathbf{F}_{n+1} - \boldsymbol{\kappa} \tilde{\mathbf{d}}_{n+1}) \quad (3.21)$$

If κ and λ is independent of position:

$$\begin{aligned} \kappa_e^{AB} &= \int_0^\ell N_{,x}^A N_{,x}^B \kappa dx \\ &= \kappa \int_0^\ell N_{,x}^A N_{,x}^B dx \\ &= \kappa \int_{-1}^{+1} N_{,\xi}^A N_{,\xi}^B \xi_{,x}^2 |J| d\xi \\ &= \kappa \frac{2}{\ell} \int_{-1}^{+1} N_{,\xi}^A N_{,\xi}^B d\xi \\ &= \pm \frac{\kappa}{\ell} = \begin{cases} +\frac{1}{2} & \text{if } A = B \\ -\frac{1}{2} & \text{if } A \neq B \end{cases} \end{aligned} \quad (3.22)$$

$$\therefore \boldsymbol{\kappa}_e = \frac{\kappa}{\ell} \begin{bmatrix} +1 & -1 \\ -1 & +1 \end{bmatrix} \quad (3.23)$$

$$M_e^{AB} = \int_0^\ell N^A N^B \lambda dx = \lambda \int_0^\ell N^A N^B dx = \frac{\lambda \ell}{2} \int_{-1}^{+1} N^A N^B dx \quad (3.24)$$

$$N^1 N^1 = \frac{1}{4} (1 - \xi)^2; N^2 N^2 = \frac{1}{4} (1 + \xi)^2; N^1 N^2 = \frac{1}{4} (1 - \xi^2) \quad (3.25)$$

$$N^1 = \frac{1 - \xi}{2}; N^2 = \frac{1 + \xi}{2} \quad (3.26)$$

Then

$$\begin{aligned}\int N^1 N^1 &= \frac{1}{4} \left[\xi + \frac{1}{3} \xi^3 \right]_{-1}^{+1} = \frac{2}{3} \\ \int N^2 N^2 &= \frac{1}{4} \left[\xi + \frac{1}{3} \xi^3 \right]_{-1}^{+1} = \frac{2}{3} \\ \int N^1 N^2 &= \frac{1}{4} \left[\xi - \frac{1}{3} \xi^3 \right]_{-1}^{+1} = \frac{1}{3}\end{aligned}\tag{3.27}$$

$$\therefore \mathbf{M}_e = \frac{\lambda \ell}{6} \begin{bmatrix} 2 & 1 \\ 1 & 2 \end{bmatrix}\tag{3.28}$$

$$\mathbf{F}_e^{fA} = \int_0^\ell N f dx = f \frac{\ell}{2} \int_{-1}^{+1} N dx = f \frac{\ell}{2} \therefore \mathbf{F}_e^f = \frac{f \ell}{2} \begin{Bmatrix} 1 \\ 1 \end{Bmatrix}\tag{3.29}$$

3.2.2 Existing Model

For this project an existing finite element model of heat diffusion by Prof. N de Koker was modified for usage in the Bayes' theorem 2.2. This model is used to determine the likelihood function. The current model uses the standard Euro code κ -values as well as the specific heat specified in the (CEN, 2004).

The model discretises the wooden element into 32 different elements. For finite element analysis, there are always more elements used to generate the model than usually evaluated. This is done to improve the accuracy of said model. The model is a one dimensional finite element model that takes time differentiation into account.

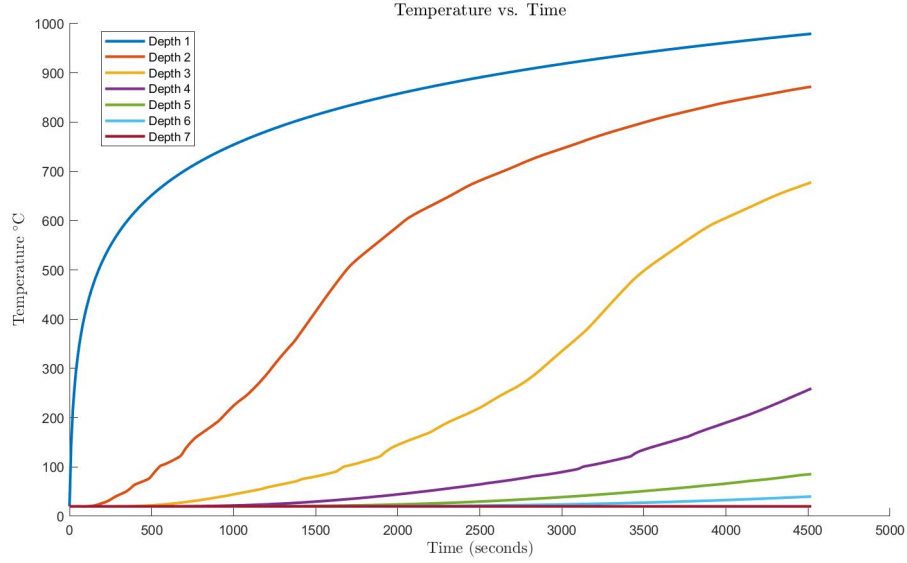


Figure 3.5: Output of finite element model using κ -values as indicated in EN 1995:1-2-2004

3.2.3 Adapted Model

The model was changed into a function that takes κ -values and provides a new temperature distribution over the elements for the different κ -values. This function is used in the posterior calculation to determine the likelihood function.

3.3 Inversion method

The basis of the stochastic analysis is the adapted Bayesian equation 3.30 below. TODO: further interpret

$$\pi^*(x|T) = \exp\left(-\frac{(\mu - x)^2}{2\sigma_\mu^2}\right) \cdot \exp\left(-\frac{(T - M(x))^2}{2\sigma_{\text{temp}}^2}\right) \quad (3.30)$$

3.3.1 Prior probability

$$\pi(x) = \exp\left(-\frac{(\mu - x)^2}{2\sigma_\mu^2}\right) \quad (3.31)$$

The prior probability function (Equation 3.31) is based on the κ -values assumed prior to any simulation or analysis. The σ_μ in this equation was assumed to be equal to 0.13 W/m·K, In this case, the prior values are indicated

as μ and refer to the vector of κ -values(3.32) at specific temperatures ?TODO how to indicate?

$$\mu = \begin{bmatrix} 0.12 \\ 0.12 \\ 0.12 \\ 0.12 \\ 0.15 \\ 0.07 \\ 0.09 \\ 0.35 \\ 1.5 \end{bmatrix} \quad (3.32)$$

The x (in Equation 3.31) refers to a vector of randomised κ -values that correspond with the same temperatures as the values in the μ vector. The first iteration of randomised κ -values are generated by creating a random perturbation of the μ vector. By multiplying the μ vector with $((0.5 + \text{rand}) \cdot 1.5)$ the first values of x are guaranteed to be within an acceptable range of the prior values. The process of obtaining the x vector after the first iteration is discussed later in section 3.3.3.

Initially the program was written to generate completely random new values for the first iteration of x . This later proved to not only be unnecessary, but also made the process less accurate as there was a larger burn-in period before the values were anywhere near the actual solution. To increase the accuracy and reduce the number of times the program needed to run to produce a sufficient number of accurate samples, the program was changed to the current method. The prior function in this case was relatively easy to generate and incorporate into the program as a well defined list of prior values exists.

3.3.2 Likelihood probability function

$$\pi(T) = \exp \left(-\frac{(T - M(x))^2}{2\sigma_{\text{temp}}^2} \right) \quad (3.33)$$

The likelihood probability was more complex to implement, as this required utilisation of the function created from the finite element model as discussed in section 3.2. This function will output the probability of the modelled values $M(x)$ given the measured temperature values (T). As can be seen in Equation 3.33, the $M(x)$ vector is written as a function. The function indicated here takes the new randomised x vector and then runs the model to provide a new temperature distribution over time at various nodes. The output of the finite element model was reduced such that only the nodes at the same depths as the thermocouples are provided to the likelihood function. For the likelihood function, the σ_{temp} value was assumed to be 15°C .

3.3.3 MCMC integration

The two main parts of the MCMC integration (as mentioned in section 2) are: how a value is deemed acceptable (Monte Carlo), and how the next random sample is selected after a previous sample is accepted (Markov Chain).

As explained in Section 2.3.1 a step size is a crucial part of determining the next random sample. For this project, a step size of 0.05 W/m·K was chosen. Compared to the example shown in Figure 2.1, the actual problem is quite more complex. For this project, a log-normal distribution was chosen instead of a uniform distribution. If every coordinate direction in the aforementioned simple example is seen as a single entry in the x vector, then the example has three κ -values. The problem also technically becomes ten-dimensional, as there are ten separate independent κ -values that must be chained. An important part of the `takesteps.m` (Appendix A) was to ensure the steps are only taken in a logical direction and that they would not move into an illogical or improbable range. Negatives were specifically forbidden, as a negative thermal diffusivity would mean that heat flows in a direction opposite to the thermal gradient.

//ALSO Write fancy code at bottom part Provision had to be made in the
//TODO

The acceptance criteria of the new x -vector is based on the proximity of the posteriori function to the reference posterior function with //TODO A potential problem encountered with the standard acceptance probability method (shown in Section 2.3.2) is that the magnitudes of the values were not considered. This problem lead to many ‘false positives’, as incorrect values were accepted even though they were not actually acceptable. TODO: add acceptance criteria

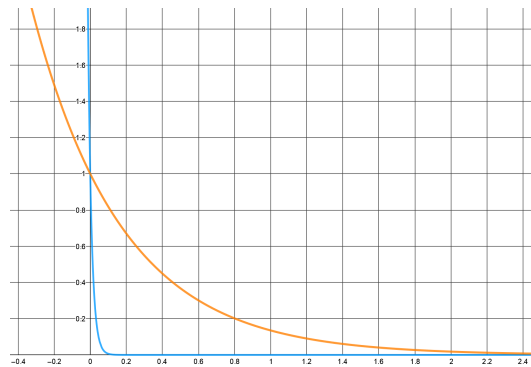


Figure 3.6: Graph explaining the difference in acceptance rates (Generated at <https://www.geogebra.org/graphing/g7kyzwce>)

Chapter 4

Results

The results of running the algorithm until 20 000 acceptable values are found is shown below.)TODO add more.

4.1 Resulting k-values

The thermal diffusivity (κ -values) at key temperatures was the main goal of this project. As can be seen in Figure 4.1 there was quite a drastic difference in the thermal diffusivity at 1200 °C and between 0 °C and 200 °C. the large difference at 1200 °C is due to hoe our model is created.(TODO?) Most of the energy at that temperature is radiated?(TODO)

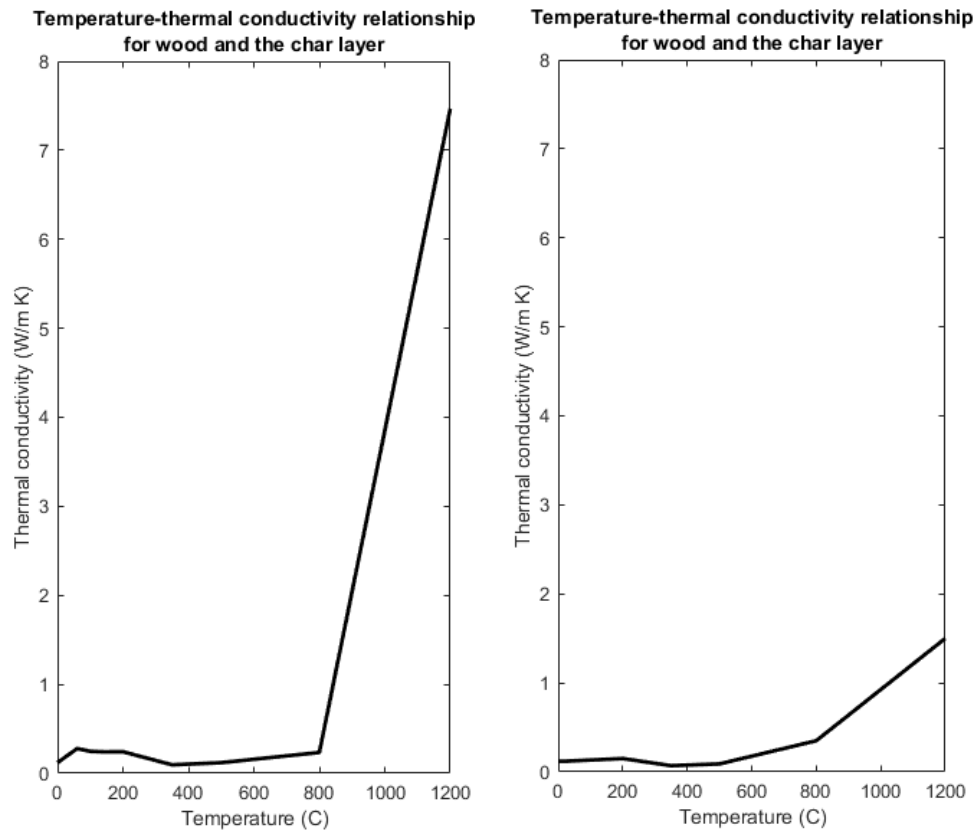
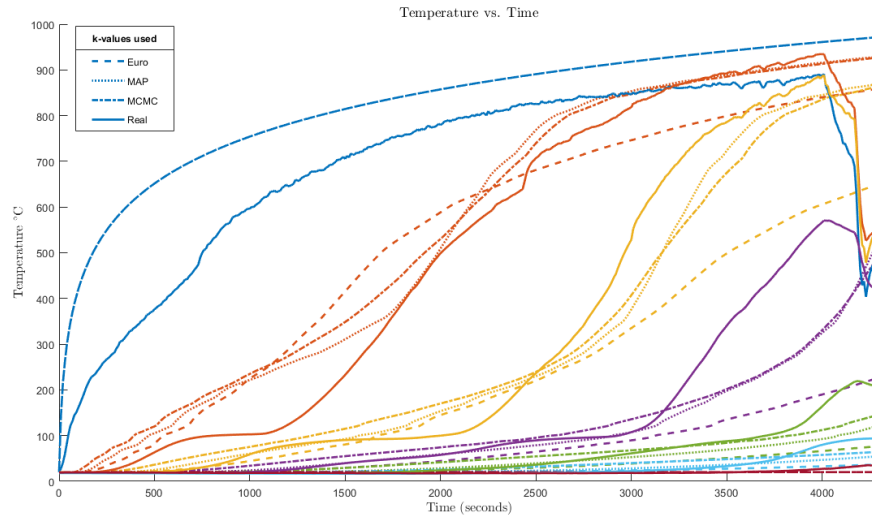


Figure 4.1: Resulting κ values (left) compared to Euro-code standard values(right)

4.2 Model output



Chapter 5

Discussion

Chapter 6

Summary and Conclusion

Further development of this concept could lead to simplified methods of calculating the fire rating of specifically SA-Pine as well as other timber samples.

Appendix A

Relevant code segments

Below are the relevant code segments taken from the Matlab code that was used to generate the final samples used for analysis.

Prior function

Determines the probability of x assuming a (NORMAL) probability over the prior values.

```
function q_val = prior_pdf(x_values,sigmaMU)

global mu_values
q_val = -0.5*((x_values - mu_values)*(x_values -
    mu_values)')/(sigmaMU^2);

end
```

Likelihood Function

```
function likelihood_pi = likelihood_func(kinput,sigmaT)

% Global variables: physical constants
global_const;
% Global variables: material properties
global_prop
% Global variables: time integration values
global_time;
% Global variables: mesh geometry
global_mesh;
% Global variables of measured temperatures
```

```

global_measuredtemp;

udepths = model_kinput(kinput);
depths_measured = [depth1;depth2;depth3;depth4;depth5;depth6;depth7];
%Where depths measure is the actual measured temperature data from
    the experiment and udepths is the temperature at the same points
    generated by the model using the new k-values.

tempmat = depths_measured - udepths;
likelihood_pi = tempmat(:)'*tempmat(:)/(-2*sigmaT^2);

end

```

Function to take next step

This function takes the current x -vector and generates a new probable x -vector.

```

function xvalue2 = takexsteps(xvalue1)
    global temps mu_values stepsize sigmastepMU sigmastepT

    locsigma = stepsize*mu_values;
    locxvalue = xvalue1 ;;

    lnMu = log(locxvalue.^2 ./ sqrt(locsigma.^2+locxvalue.^2));
    lnSigma = sqrt(log(locsigma.^2./xvalue1.^2 + 1));

    xvalue2 = max(0, lognrnd(lnMu, lnSigma));
    xvalue2(1) = xvalue1(1);

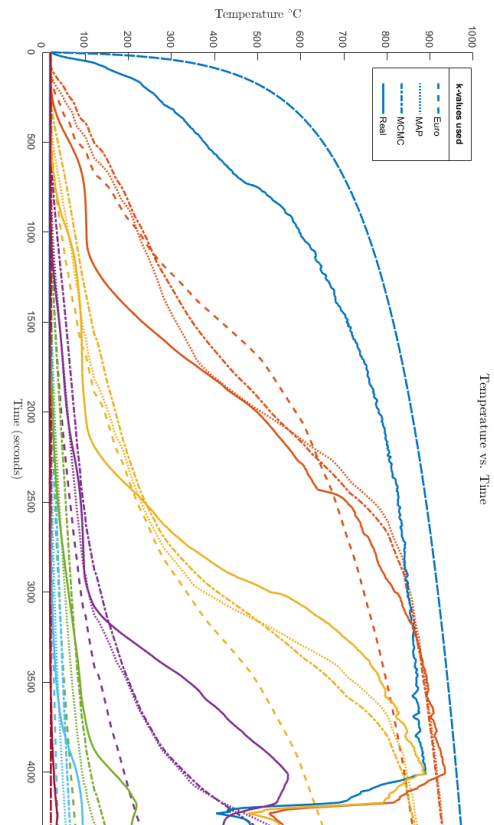
    xvalue2(xvalue2<locsigma/20) =
        (mu_values(xvalue2<locsigma/20)+xvalue2(xvalue2<locsigma/20))/2;

end

```

Appendix B

Detailed results graph



Appendix C

Derivation

More generally matrix K_e and M_e are:

$$\begin{aligned} K_e^{AB} &= \int_0^\ell N_{,x}^A N_{,x}^B \kappa dx \text{ with } \kappa = N^1 \kappa^1 + N^2 \kappa^2 \\ &= \left(\frac{\ell}{2}\right) \left(\frac{\pm 1}{4}\right) \left(\frac{4}{\ell^e}\right) \int_{-1}^{+1} \left[\frac{1-\xi}{2} \kappa^{(1)} + \frac{1+\xi}{2} \kappa^{(2)} \right] d\xi \end{aligned} \quad (C.1)$$

and

$$M_e^{AB} = \int_0^\ell N^A N^B \lambda dx \quad \text{with} \quad \lambda = N^1 \kappa^{(1)} + N^2 \kappa^{(2)} \quad (C.2)$$

If $A = 1$ and $B = 1$ then M_e is calculated as shown below in Equation C.3.

$$\begin{aligned} M_e^{11} &= \left(\frac{\ell}{2}\right) \int_{-1}^{+1} \frac{1}{4} (1-\xi)^2 \left[\frac{1-\xi}{2} \cdot \lambda^{(1)} + \frac{1+\xi}{2} \cdot \lambda^{(2)} \right] d\xi \\ &= \frac{\ell}{16} \int_{-1}^{+1} [(1-\xi)^2 (1-\xi) \lambda^{(1)} + (1-\xi)^2 (1+\xi) \lambda^{(2)}] d\xi \\ &= \frac{\ell}{16} \left[\lambda^{(1)} \int_{-1}^{+1} (1-\xi)^2 (1-\xi) d\xi + \lambda^{(2)} \int_{-1}^{+1} (1-\xi)^2 (1+\xi) d\xi \right] \quad (C.3) \\ &= \frac{\ell}{16} \left[\lambda^{(1)} \cdot 4 + \lambda^{(2)} \cdot \frac{4}{3} \right] \\ &= \frac{\ell}{4} \left[\lambda^{(1)} + \frac{\lambda^{(2)}}{3} \right] \end{aligned}$$

When $A = 2$ and $B = 2$:

$$\begin{aligned} M_e^{22} &= \frac{\ell}{16} \int_{-1}^{+1} [(1+\xi)^2 (1-\xi) \lambda^{(1)} + (1+\xi)^2 (1+\xi) \lambda^{(2)}] d\xi \\ &= \frac{\ell}{4} \left[\frac{\lambda^{(1)}}{3} + \lambda^{(2)} \right] \end{aligned} \quad (C.4)$$

When $A = 1$ and $B = 2$ or $A = 2$ and $B = 1$:

$$\begin{aligned}
 M_e^{12} &= \frac{\ell}{16} \int_{-1}^{+1} [(1 - \xi^2)(1 - \xi)\lambda^{(1)} + (1 - \xi^2)(1 + \xi)\lambda^{(2)}] d\xi \\
 &= \frac{\ell}{4} \left[\frac{\lambda^{(1)}}{3} + \frac{\lambda^{(2)}}{3} \right] \\
 &= \frac{\ell}{12} [\lambda^{(1)} + \lambda^{(2)}]
 \end{aligned} \tag{C.5}$$

The matrix can then be assembled from the above Equations C.3, C.4 and C.5:

$$\begin{aligned}
 \mathbf{M}_e &= \frac{\ell}{4} \left(\lambda^{(1)} \begin{bmatrix} 1 & \frac{1}{3} \\ \frac{1}{3} & \frac{1}{3} \end{bmatrix} + \lambda^{(2)} \begin{bmatrix} \frac{1}{3} & \frac{1}{3} \\ \frac{1}{3} & 1 \end{bmatrix} \right) \\
 &= \frac{\ell}{12} \left(\lambda^{(1)} \begin{bmatrix} 3 & 1 \\ 1 & 1 \end{bmatrix} + \lambda^{(2)} \begin{bmatrix} 1 & 1 \\ 1 & 3 \end{bmatrix} \right)
 \end{aligned} \tag{C.6}$$

The same can be done to assemble the K matrix as shown below.

$$\begin{aligned}
 K_e^{AB} &= \left(\frac{\pm 1}{2\ell} \right) \int_{-1}^{+1} \left[\frac{1 - \xi}{2} \kappa^{(1)} + \frac{1 + \xi}{2} \kappa^{(2)} \right] d\xi \\
 &= \left(\frac{\pm 1}{2\ell} \right) [\kappa^{(1)} + \kappa^{(2)}]
 \end{aligned} \tag{C.7}$$

$$\mathbf{K}_e = \frac{1}{2\ell} \left(\kappa^{(1)} \begin{bmatrix} 1 & -1 \\ -1 & 1 \end{bmatrix} + \kappa^{(2)} \begin{bmatrix} 1 & -1 \\ -1 & 1 \end{bmatrix} \right) \tag{C.8}$$

There after the \mathbf{F}_e matrix

$$\begin{aligned}
 F_e^A &= \int_0^\ell N^A f dx \\
 &= \frac{\ell}{2} \int_{-1}^{+1} N^A f d\xi
 \end{aligned} \tag{C.9}$$

$$\begin{aligned}
 F_e^1 &= \frac{\ell}{2} \int_{-1}^{+1} \left(\frac{1 - \xi}{2} \right) \cdot \left[\frac{1 - \xi}{2} \cdot f^{(1)} + \frac{1 + \xi}{2} \cdot f^{(2)} \right] \\
 &= \frac{\ell}{8} \int_{-1}^{+1} [(1 - \xi)^2 \cdot f^{(1)} + (1 - \xi^2) \cdot f^{(2)}] d\xi
 \end{aligned} \tag{C.10}$$

$$F_e^2 = \frac{\ell}{8} \int_{-1}^{+1} [(1 - \xi^2) \cdot f^{(1)} + (1 + \xi)^2 \cdot f^{(2)}] d\xi \tag{C.11}$$

$$\begin{aligned}
\therefore \mathbf{F}_e &= \frac{\ell}{8} \left(f^{(1)} \begin{Bmatrix} 8 \\ 3 \\ 4 \\ 3 \end{Bmatrix} + f^{(2)} \begin{Bmatrix} 4 \\ 8 \\ 3 \\ 3 \end{Bmatrix} \right) + \sum_{A \in \mathcal{A}_N} q^{(A)} \begin{Bmatrix} -\delta^{A1} \\ +\delta^{A2} \end{Bmatrix} \\
&= \frac{\ell}{6} \left(f^{(1)} \begin{Bmatrix} 2 \\ 1 \end{Bmatrix} + f^{(2)} \begin{Bmatrix} 1 \\ 2 \end{Bmatrix} \right) + \sum_{A \in \mathcal{A}_N} q^{(A)} \begin{Bmatrix} -\delta^{A1} \\ +\delta^{A2} \end{Bmatrix}
\end{aligned} \tag{C.12}$$

TODO: uppercase or lowercase A1 and A2 with deltas?

After assembly but before Dirichlet boundaries are applied

$$\bar{\mathbf{c}}^T \bar{\mathbf{K}} \bar{\mathbf{d}} + \bar{\mathbf{c}}^T \bar{\mathbf{M}} \dot{\bar{\mathbf{d}}} = \bar{\mathbf{c}}^T \bar{\mathbf{F}} \tag{C.13}$$

When the Dirichlet boundaries below (Equation C.14) are applied to the matrices shown in Equation C.13, they can be simplified to Equation C.15.

$$\begin{aligned}
c_1 &= 0 \quad \text{and} \quad c^{np} = 0 \\
d_1 &= u_{\text{fire}(t)} \quad \text{and} \quad d^{np} = u_{\text{air}}
\end{aligned} \tag{C.14}$$

Then:

$$\mathbf{c}^T \cdot \mathbf{K} \cdot \mathbf{d} + \mathbf{c}^T \cdot \mathbf{M} \cdot \dot{\mathbf{d}} = \mathbf{c}^T \cdot \mathbf{F}' - \mathbf{c}^T (\{K'\}d' + \{K^{np?}\}d^{np?}) - \mathbf{c}^T (\{M'\}\dot{d}' + \{M^{np?}\}\dot{d}^{np?}) \tag{C.15}$$

And so:

$$\mathbf{K} \cdot \mathbf{d} + \mathbf{M} \cdot \dot{\mathbf{d}} = \mathbf{F}' - \mathbf{F}^{Ke?} - \mathbf{F}^{Me?} = \mathbf{F} \tag{C.16}$$

Solve as

$$\begin{aligned}
\tilde{\mathbf{d}}_{n+1} &= \mathbf{d}_n + (1 - \alpha)\Delta t \mathbf{v}_n \\
(\mathbf{M} + \alpha\Delta t \mathbf{K})\mathbf{v}_{n+1} &= \mathbf{F}_{n+1} - \mathbf{K}\tilde{\mathbf{d}}_{n+1} \\
\rightarrow \mathbf{v}_{n+1} &= (\mathbf{M} + \alpha\Delta t \mathbf{K})^{-1}(\mathbf{F}_{n+1} - \mathbf{K}\tilde{\mathbf{d}}_{n+1}) \\
\rightarrow \mathbf{d}_{n+1} &= \tilde{\mathbf{d}}_{n+1} + \alpha\Delta t \mathbf{v}_{n+1} \\
\mathbf{v} &= \dot{\mathbf{d}}
\end{aligned} \tag{C.17}$$

Appendix D

Program

Date	What should be done before then
4 Jun	Topic allocated. Contact study leader
23 Jun - 31 Jul	Exams and Recess
10 Aug - 23 Aug	Work on Introduction and Literature study for project proposal
24 Aug	Submit project proposal
25 Aug - 2 Sep	Familiarize with FEM model and MCMC process
2 - 10 Sep	Begin coding a basic MCMC process
10 - 17 Sep	Testweek, minimal time can be allotted to skripsie
18 - 30 Sep	Work on MCMC code during recess
1-8 Oct	Finalise Matlab program for MCMC analysis
8-10 Oct	Run simulation
10 - 17 Oct	Add results, discussion of result and conclusion to report
18 Oct	Submit final draft report
20 - 28 Oct	Finalise report and correct as suggested by study leader
28 - 30 Oct	Print and bind report
1 Nov	Submit report

Appendix E

GA outcomes

GA1: Problem Solving

In Chapter 1 the problem as well as the relevant aims and objectives are explained. The problem is approached systematically and a solution is proposed in Chapter 3.

GA2: Application of scientific and engineering knowledge

The problem tackled in this project was mathematically and statistically complex. The report was laid out in a way that would make sense to the reader even if they had minimal understanding of the MCMC algorithm. The limitations of this project were presented in Chapter 5.(TODO)

GA4: Investigations,experiments and data analysis

An overview of the available knowledge and previous studies on the matter is presented in Section 1.3. Multiple versions of the final algorithm were considered, corrected and fine-tuned. The results are analysed and discussed in Chapter 4 and 5. A final conclusion was draw and presented in Chapter 6.

GA5: Engineering methods , skill and tools, including IT

The following subjects were directly relevant and needed for the completion of this project:

- Informatics 244, 314;
- Applied Mathematics 252;
- Engineering Statistics 314;
- Engineering Mathematics 115, 145, 214;

List of References

- Brownlee, J. (2019 Nov [Online]). A gentle introduction to markov chain monte carlo for probability. Machine Learning Mastery, Blog.
Available at: <https://machinelearningmastery.com/markov-chain-monte-carlo-for-probability/>
- CEN (2004). *BS EN 1995-1-2:2004. Eurocode 5: Design of timber structures - General - Structural fire design*. BSI, London.
- Cook, J.D. (2016 Jan [Online]). MCMC burn-in. John D. Cook Consulting.
Available at: <https://www.johndcook.com/blog/2016/01/25/mcmc-burn-in/comment-page-1/?unapproved=1094214&moderation-hash=912d585bd365341b032df1d4f1bddf3b#comment-1094214>
- Courant, R. (1943). Variational methods for the solution of problems of equilibrium and vibrations. *Bulletin of the American Mathematical Society*, pp. 1–23. ISSN 1088-9485.
Available at: <https://doi.org/10.1090/S0002-9904-1943-07818-4>
- Fish, J.J. (2007). *A first course in finite elements*. John Wiley, Chichester. ISBN 9780470035801.
- Frayssinhes, R., Girardon, S., Marcon, B., Denaud, L. and Collet, R. (2020). A simple method to determine the diffusivity of green wood. *BioRes*, vol. 3, no. 15, pp. 6539–6549.
- Gilks, W.R., Richardson, S. and Spiegelhalter, D.J. (1996). *Markov chain Monte Carlo in practice*. London, 1st edn.
- Gupta, K. and Meek, J. (1996). A brief history of the beginning of the finite element method. *International Journal for Numerical Methods in Engineering*, vol. 39, pp. 3761–3774.
- ISO (1999). *ISO 834 Fire-resistance test - Elements of building construction*. International Organization for Standardization, Geneva.
- Kaipio, J. and Somersalo, E. (2005). *Statistical and Computational Inverse Problems*. Verlag New York.

- Meyn, S. and Tweedie, R. (1993 Jan). *Markov Chains and Stochastic Stability*, vol. 92. Springer Verlag.
- Robert, C.P. and Casella, G. (2004). *Monte Carlo Statistical Methods*, vol. 42. 2nd edn. Springer New York. ISBN 9781441919397.
- Salvadori, V. (2017 12). *The Development of a Tall Wood Building*. Master's thesis, Polytechnic University of Milan and TU Wien.
- Shi, L. and Chew, M.Y.L. (2021 Aug). A review of thermal properties of timber and char at elevated temperatures. *Indoor and Built Environment*, pp. 1–16. <https://doi.org/10.1177/1420326X211035557>.
Available at: <https://doi.org/10.1177/1420326X211035557>
- van der Westhuyzen, S., Walls, R. and de Koker, N. (2020). Fire tests of south african cross-laminated timber wall panels: Fire ratings, charring rates, and delamination. *Journal of the South African Institution of Civil Engineering*, vol. 62, no. 1, pp. 33–41. ISSN 23098775.
- Wiecki, T. (2015 Nov [Online]). MCMC sampling for dummies. While My MCMC Gently Samples, Blog.
Available at: <https://twiecki.io/blog/2015/11/10/mcmc-sampling/>